

ARTICLE

Received 1 Apr 2010 | Accepted 8 Jun 2011 | Published 5 Jul 2011

DOI: 10.1038/ncomms1377

Tonic excitation or inhibition is set by GABA_A conductance in hippocampal interneurons

Inseon Song¹, Leonid Savtchenko² & Alexey Semyanov¹

Inhibition is a physiological process that decreases the probability of a neuron generating an action potential. The two main mechanisms that have been proposed for inhibition are hyperpolarization and shunting. Shunting results from increased membrane conductance, and it reduces the neuron-firing probability. Here we show that ambient GABA, the main inhibitory neurotransmitter in the brain, can excite adult hippocampal interneurons. In these cells, the GABA_A current reversal potential is depolarizing, making baseline tonic GABA_A conductance excitatory. Increasing the tonic conductance enhances shunting-mediated inhibition, which eventually overpowers the excitation. Such a biphasic change in interneuron firing leads to corresponding changes in the GABA_A-mediated synaptic signalling. The described phenomenon suggests that the excitatory or inhibitory actions of the current are set not only by the reversal potential, but also by the conductance.

¹RIKEN Brain Science Institute (BSI), Wako, Saitama 351-0198, Japan. ² Department of Clinical and Experimental Epilepsy, UCL Institute of Neurology, London WC1N 3BG, UK. Correspondence and requests for materials should be addressed to A.S. (email: semyanov@brain.riken.jp).

GABA is the main inhibitory neurotransmitter in the adult brain. Synaptically released GABA activates postsynaptic GABA_A receptors, which trigger fast inhibitory postsynaptic currents (IPSCs). Ambient GABA produces persistent activation of extrasynaptic GABA_A receptors, which are responsible for the tonic current^{1–3}. The tonic current is mediated by heterogeneous and plastic GABA_A receptors^{4,5} and is expressed in a cell-type specific manner in various brain structures, such as the hippocampus⁶, thalamus⁷, neocortex⁸ and striatum⁹. Cell type-specific expression of the tonic current indicates the importance of this phenomenon for neuronal network operation, especially when the extracellular GABA concentration changes. Indeed, changes in ambient GABA levels are reported in both physiological (for example, during exploratory behaviour) and pathological (for example, epilepsy, pain) conditions^{10–12}.

The effect of GABA on cell excitability is largely determined by the reversal potential for Cl[−], which is the major ion responsible for the GABA_A current. In adult neurons, the intracellular Cl[−] concentration is kept low by developmentally regulated cotransporters^{13,14} and sets a reversal potential for GABA_A currents (E_{GABA}) close to the resting membrane potential (RMP). The RMP and E_{GABA} vary among cell types and even cell compartments^{15,16}; therefore, the effect of GABA can be either hyperpolarizing or depolarizing. Whereas hyperpolarization is the primary synaptic action of GABA on cortical principal neurons¹⁷, depolarizing effects of GABA are observed in interneurons in numerous circuits, including the hippocampus^{18–21}, cerebellum²², and basolateral amygdala²³; as well as in striatal neurons^{9,24} and peripheral nervous system neurons²⁵. Because this depolarization is set by a small driving force for Cl[−], the predominant effect of GABA_A activation is thought to be shunting inhibition.

Shunting inhibition is a conductance-dependent phenomenon and may not provide strong inhibitory effects on the cell at low GABA_A conductances. In contrast, even a small depolarization of the neuronal membrane can trigger activation of some voltage dependent channels. In turn, activation of these channels can potentially bring the RMP to the action potential threshold. This raises the possibility that low depolarizing GABA_A conductance can be excitatory whereas high conductance is inhibitory though shunting²⁶. Previous reports suggested that voltage-dependent oscillations of the membrane potential in hippocampal interneurons could reach the action potential threshold and trigger cell firing^{27–29}. Indeed, hippocampal CA1 *stratum (str.) radiatum* interneurons could fire spontaneous action potentials even when excitatory neurotransmission was blocked. Here we found that the firing frequency of these cells is bidirectionally regulated by ambient GABA concentrations. Low GABA concentrations increased both membrane potential fluctuations and cell firing; high concentrations decreased these two parameters below the control values.

Results

Biphasic effect of tonic conductance on interneuron firing. We investigated the effect of tonic GABA_A conductance on CA1 *str. radiatum* interneurons in mouse hippocampal slices and blocked ionotropic glutamate and GABA_B receptors. Consistent with previous reports, gramicidin-perforated patch recordings showed that these cells have depolarizing E_{GABA} (RMP, -71.4 ± 2.7 mV $n = 5$; E_{GABA} , -62.4 ± 2.7 , $n = 5$, $P = 0.003$ paired t -test; Fig. 1a,b)^{18–21}. As expected, exogenous GABA produced a concentration-dependent increase in the tonic GABA_A conductance (Δg_{GABA} , 0.41 ± 0.08 nS, 0.72 ± 0.09 nS, and 1.55 ± 0.34 nS for 1, 5, and 50 μM GABA, respectively, $n = 8$; Fig. 1c,d)^{3,6}. In cell-attached recordings, the interneurons could fire spontaneous action potentials despite the blockade of ionotropic glutamate receptors (Supplementary Fig. S1). In contrast to the commonly held notion that GABA mediates inhibitory tonic conductance^{1,2,30}, however, 1 μM GABA increased

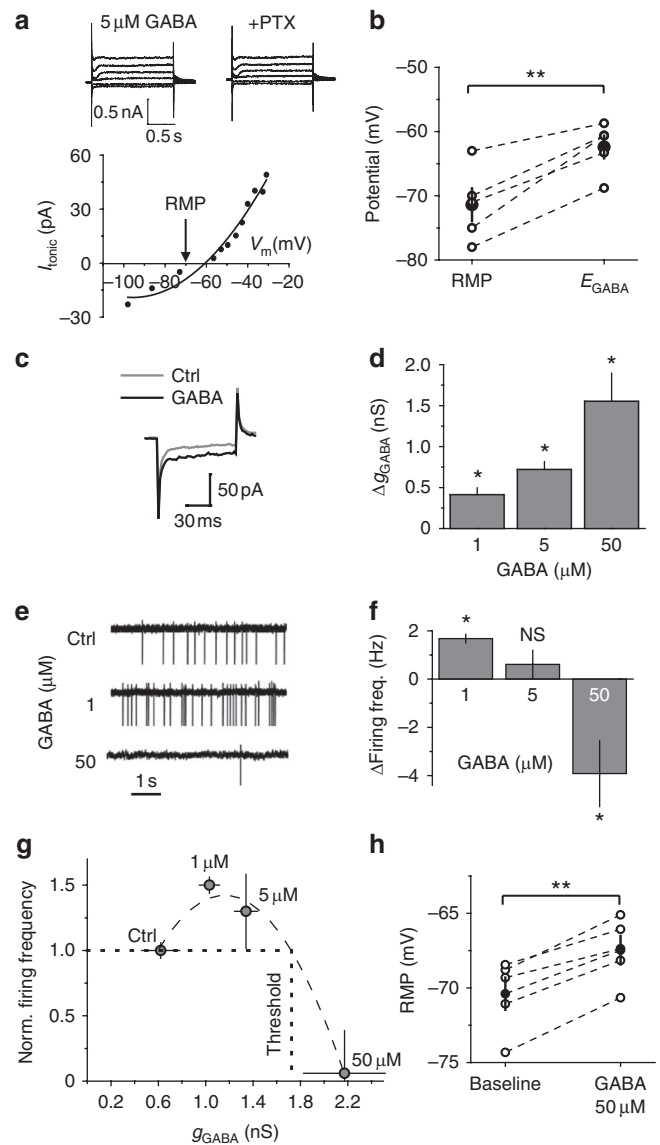


Figure 1 | The effect of ambient GABA on interneuron membrane

properties and firing. (a) Top, Gramicidin-perforated patch recordings at voltage steps from -90 to -20 mV in $5 \mu\text{M}$ GABA and, thereafter $100 \mu\text{M}$ picrotoxin (+PTX) was added. Tonic GABA_A currents at different voltages were calculated by subtracting the '+PTX'-currents from corresponding ' $5 \mu\text{M}$ GABA'-currents. Bottom: Tonic current (I_{tonic}) versus membrane potential (V_m). Points were fitted with a second-order polynomial function to determine E_{GABA} . Arrow marks RMP. (b) Summary data of RMP and E_{GABA} showing data from individual cells ($n = 5$, empty circles) and mean values (black circles). (c) Five averaged current traces induced by -5 mV voltage step in control (ctrl) and in $50 \mu\text{M}$ GABA, demonstrating change in membrane conductance. (d) Summary plot of the GABA-induced change in membrane conductance (Δg_{GABA}) ($n = 7$ for $1 \mu\text{M}$ GABA, $n = 5$ for $5 \mu\text{M}$ GABA, $n = 5$ for $50 \mu\text{M}$ GABA). (e) Cell-attached recordings from interneurons in control and in 1 and $50 \mu\text{M}$ GABA. (f) Summary plot of the change in firing frequency induced by GABA. (g) Summary plot of normalized firing frequency versus tonic GABA_A conductance (g_{GABA}) with a second order polynomial fit (dashed line). Dotted lines indicate the threshold conductance. (h) Effect of $50 \mu\text{M}$ GABA on RMP in individual cells ($n = 5$, empty circles) and mean values (black circles). Error bars, s.e.m., $^{***}P < 0.005$, $^{**}P < 0.05$, NS $P > 0.05$, paired t -test.

interneuron firing by 1.68 ± 0.18 Hz ($n=7$, $P=0.028$ paired t -test). Cell firing did not significantly change with $5 \mu\text{M}$ GABA (increase by 0.6 ± 0.6 Hz, $n=5$, $P=0.2$ paired t -test), and significantly decreased with $50 \mu\text{M}$ GABA by 3.9 ± 1.3 Hz ($n=5$, $P=0.023$ paired t -test; Fig. 1e,f). These findings suggest a biphasic effect of tonic GABA_A conductance on cell excitability. Therefore, we established the inhibitory threshold conductance at which GABA switches its action from excitatory to inhibitory and the peak excitation conductance at which GABA produces maximal excitatory effect. We plotted the cell firing rate versus the corresponding tonic GABA_A conductance ($g_{\text{GABA}} = \text{baseline tonic conductance} + \Delta g_{\text{GABA}}$). The inhibitory threshold conductance (1.73 nS) and the peak excitation conductance (1.16 nS) were obtained from a second-order polynomial fit (Fig. 1g). These two parameters characterize the cell response to the change in ambient GABA concentration and are potentially important for computation within individual interneurons and local networks.

According to the above definition of the peak excitation conductance an increase in the tonic GABA_A conductance further from this point should decrease the cell firing rate and vice versa. Indeed, a low dose of the GABA_A antagonist picrotoxin ($1 \mu\text{M}$) reversed the inhibitory effect of $10 \mu\text{M}$ GABA by partial reduction of the tonic GABA_A conductance, presumably setting it closer to the peak excitation (Supplementary Fig. S2). It should be noted that picrotoxin at this concentration has only a minor effect on IPSCs⁶. This finding is consistent with our previous report demonstrating an increase in hippocampal interneuron firing in guinea pigs by partially reducing the tonic conductance⁶. Baseline tonic GABA_A conductance in guinea pig interneurons is almost twice that in mice (guinea pigs, 1.1 ± 0.3 nS, $n=7$ versus mice, 0.62 ± 0.16 nS, $n=7$)⁶ and could be above the excitation peak conductance in these animals, even if still below the inhibitory threshold conductance (excitatory GABA action).

The inactivation of Na⁺ channels is an alternative explanation for the biphasic effect of tonic GABA_A depolarization. This explanation for the inhibitory effect of depolarizing GABA was previously suggested for neurons in the peripheral nervous system³¹. In fact, GABA could not provide strong depolarization to hippocampal interneurons, even at high conductances ($E_{\text{GABA}} \sim 10$ mV above RMP). $50 \mu\text{M}$ GABA produced only 3.1 ± 0.1 mV ($n=5$, $P=0.001$ paired t -test) of depolarization in perforated-patch experiments (Fig. 1h). In whole-cell current clamp recordings, we tested the effect of a depolarizing block on the interneuron firing by injecting different amounts of constant current. At first, cell firing increased with the depolarization, but after the depolarization reached -38.7 ± 4.1 mV (~ 26 mV above RMP, $n=5$), the firing rate began to decrease, presumably due to inactivation of Na⁺ channels. This finding indicates that the small amount of depolarization produced by ambient GABA is unlikely to produce a significant depolarizing block in hippocampal interneurons. We cannot completely rule out this possibility, however, because the depolarizing effect of GABA can be larger in the axon initial segment, as it has been demonstrated in principle cells in the context of axo-axonic synaptic connections^{16,32}.

The small depolarization produced by tonic GABA_A conductances raises the question that whether it is sufficient to reach the action potential threshold. Consistent with previous reports, the action potential threshold (the value of membrane potential when the first derivative of potential was 30 mV/ms) estimated in whole-cell current clamp recordings was -43.9 ± 2.3 mV ($n=8$)²⁷. Indeed, the small depolarization produced by tonic GABA_A conductance cannot reach this value. The action potential measurements, however, are commonly obtained in the cell soma although the action potential threshold can be lower in the axon trigger zone. Moreover, neuron firing can be triggered not by constant depolarization, but through the enhancement of voltage-dependent membrane potential fluctuations charac-

teristic of interneurons^{29,33}. Indeed, GABA produced a biphasic effect on the standard deviation (s.d.) of the RMP recorded in perforated-patch experiments: $1 \mu\text{M}$ GABA increased s.d. by $25 \pm 8\%$ ($n=5$, $P=0.04$ paired t -test), $5 \mu\text{M}$ produced an insignificant decrease of $10 \pm 10\%$ ($n=7$, $P=0.19$, paired t -test), and $50 \mu\text{M}$ decreased the s.d. by $24 \pm 9\%$ ($n=6$, $P=0.03$ paired t -test). The observed decrease in the RMP fluctuations produced by $50 \mu\text{M}$ GABA was consistent with the previously reported observations in cell attached recordings²¹.

Thus, our results point that low tonic GABA_A conductance depolarizes the cell and enhances voltage-dependent fluctuations of the RMP, which can trigger action potentials. When the conductance increases, however, it shunts the fluctuations and prevents cell firing. If this is the case, such a mechanism should work not only in hippocampal interneurons, but also in any neuron with depolarizing GABA. We addressed this issue by developing a simple computer simulation on a cylindrical model cell lacking any interneuron-specific features. The excitability of this cell was based on the Hodgkin-Huxley model with the kinetics of Na⁺ and K⁺ channels assuming stochastic opening and closing (Methods). The cell also contained stochastic A-type K⁺ channels³⁴. Under baseline conditions, the cell received no synaptic input and generated no action potentials, but did show small fluctuations in the RMP (Fig. 2a). A tonic GABA_A conductance ($g_{\text{GABA}} = 0-0.2$ mS cm⁻²) with depolarizing E_{GABA} (10.2 mV above RMP) was then introduced. This produced a biphasic change in the cell firing frequency that was dependent on the g_{GABA} amplitude, similar to the effect observed in hippocampal interneurons (Fig. 2a,b). The density of Na⁺ channels was then reduced from $50 \mu\text{m}^{-2}$ (in initial model) to $25 \mu\text{m}^{-2}$ to prevent the model cell from spiking, which allowed us to observe the effect of g_{GABA} on the RMP fluctuations (Fig. 2c). The RMP s.d. initially increased with cell depolarization, and then decreased regardless of the membrane potential (Fig. 2d). Interestingly, the biphasic changes in the cell firing frequency and in the RMP fluctuations were not due to the inactivation of Na⁺ channels. The depolarizing current injections did not produce any biphasic effect on the above parameters at the same RMP range that was produced by g_{GABA} (Fig. 2e-h). This model demonstrates that the described phenomenon does not require any specific cell anatomy, subcellular gradients of E_{GABA} , or inactivation of Na⁺ channels; and can be achieved with a limited number of voltage-dependent conductances.

Synaptic GABA_A currents are inhibitory. Our findings suggest that whereas a low tonic GABA_A conductance can be excitatory, synaptic signalling mediated by high GABA_A conductance should provide shunting inhibition in hippocampal interneurons. To test this, we produced stimulations with an extracellular electrode placed proximally to the recorded cell in the *str. radiatum*. The recordings were performed in the presence of ionotropic glutamate and GABA_B receptor antagonists. First, in whole-cell mode, we recorded the evoked GABA_A-mediated postsynaptic current (PSC) induced in CA1 interneurons by $50\text{-}\mu\text{A}$, $200\text{-}\mu\text{s}$ stimulus (Supplementary Fig. S3). We then estimated the postsynaptic conductance (PSG) required to generate such a PSC according using the following formula: $\text{PSG} = \text{PSC} / (E_{\text{GABA}} - V_{\text{hold}})$, where V_{hold} is the holding potential (-70 mV). The PSG peak conductance 4.6 ± 0.8 nS ($n=7$, Fig. 3a) was significantly larger than the conductance required to reach the inhibitory threshold conductance from the baseline tonic GABA_A conductance (1.1 nS, calculated as the difference between the inhibitory threshold conductance and baseline tonic GABA_A conductance, Fig. 1g). Moreover, the synaptic conductance calculated from PSCs, recorded in the soma, was probably underestimated because some synaptic currents originate from the distal dendrites. Second, we recorded CA1 interneuron firing in the cell-attached mode and produced extracellular stimulation as described above. The time between the stimulus and preceding spike (t_{ps}) was assumed to be

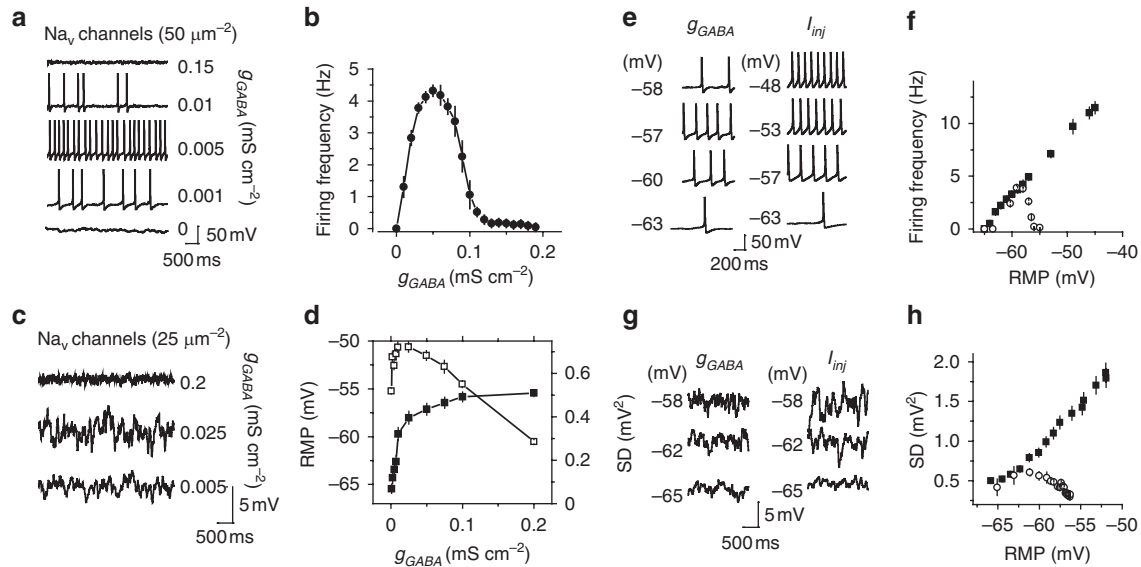


Figure 2 | The effect of depolarizing tonic GABA_A conductance on a model neuron. (a) Sample traces of the cell firing induced by g_{GABA} . (b) Summary plot of the cell firing frequency versus g_{GABA} ($n = 10$). (c) Sample traces of the effect of g_{GABA} on RMP fluctuations set by stochastic channel openings. The Na⁺ channel density was reduced by half compared with panel a to avoid cell firing. (d) Summary plot of RMP (black squares, $n = 10$) and RMP standard deviation (s.d., white squares, $n = 10$) versus g_{GABA} . (e) Representative traces of membrane potential at different RMPs produced by g_{GABA} (left panel) and by I_{inj} (right panel). (f) Summary data of the change in the model cell firing at different RMPs set by g_{GABA} (empty circles, $n = 10$) and by I_{inj} (black squares, $n = 10$). (g) Representative traces of membrane potential at different RMPs produced by g_{GABA} (left panel) and by I_{inj} (right panel). g_{Na} was reduced by half to prevent the cell from firing. (h) Mean standard deviation of RMP (s.d.) at different RMPs set by g_{GABA} (empty circles, $n = 10$) and by I_{inj} (black squares, $n = 10$). Error bars, s.e.m.

random; the time between the stimulus and the succeeding spike (t_{ss}) was influenced by the PSG. The mean t_{ps} and t_{ss} were compared for each cell (Fig. 3b). Consistent with the inhibitory synaptic effect, the t_{ss} was almost twice as large as the t_{ps} ($t_{\text{ss}}/t_{\text{ps}}$, 1.96 ± 0.55 , $n = 6$, $P = 0.011$ paired t -test). The difference between t_{ps} and t_{ss} was completely blocked by $100 \mu\text{M}$ picrotoxin ($t_{\text{ss}} - t_{\text{ps}}$, 126 ± 14.7 ms in control and -7.8 ± 35 ms in picrotoxin, $n = 5$, $P = 0.02$ paired t -test; Fig. 3c). These data support the notion that GABA_A-mediated PSGs in interneurons are inhibitory (IPSGs). Therefore, we use the term spontaneous inhibitory PSCs (sIPSCs) in the following sections for consistency. An alternative explanation for the inhibitory effect of synaptic GABA is that the site of action is different from that of tonic conductance. In a separate set of experiments, we tested the effect of a GABA puff ($100 \mu\text{M} \times 100$ ms). Similar to synaptic stimulation, the GABA puff increased the t_{ss} by a factor of two ($t_{\text{ss}}/t_{\text{ps}}$, 1.99 ± 0.31 , $n = 4$, $P = 0.005$ paired t -test; Fig. 3d). Because puff application produces a local transient increase in GABA, which activates both synaptic and extrasynaptic GABA_A receptors, this finding suggests that the conductance magnitude is more important than the site of action.

Biphasic changes in GABAergic synaptic signalling. Tonic GABA_A conductance is commonly referred as ‘tonic inhibition’^{21,2,30} and therefore its function in neuronal networks is thought to be unidirectional. Here we demonstrate that tonic GABA_A conductance has a biphasic effect on the hippocampal interneuron firing rate. Interneurons are a diverse group of cells and each class of interneurons has a different function in the local network³⁵. The amount of tonic GABA_A conductance also varies among interneuron types⁸. Thus, our sample of interneurons does not characterize the tonic GABA_A current in all classes of interneurons and cannot be used to predict the effect of ambient GABA on the CA1 network. Therefore, we recorded the sIPSC frequency directly in CA1 pyramidal neurons, which are the final targets of the CA1 interneurons and generate the major hippocampal output.

Consistent with the biphasic change in interneuron firing, $1 \mu\text{M}$ GABA increased sIPSC frequency in the pyramidal cells by 1.5 ± 0.5 Hz ($n = 11$, $P = 0.005$ paired t -test), $5 \mu\text{M}$ GABA did not produce a significant change (increase by 0.25 ± 0.55 Hz; $n = 9$, $P = 0.34$ paired t -test), and $50 \mu\text{M}$ GABA reduced the frequency by 1.2 ± 0.4 Hz ($n = 6$, $P = 0.036$ paired t -test; Fig. 4a,b). In this set of experiments, we used relatively high concentrations of exogenous GABA (up to $50 \mu\text{M}$). Although it is unlikely that all the GABA reached the neurons deep in the tissue because of its efficient uptake, it is still possible that some of the synaptic GABA_A receptors were recruited or desensitized, and the activation of presynaptic GABA_A receptors affected the probability of GABA release. To rule out these possibilities, we recorded action-potential independent miniature IPSCs (mIPSCs) under control conditions in the presence of $1 \mu\text{M}$ tetrodotoxin (Na⁺ channel blocker) and then added 1, 5 or $50 \mu\text{M}$ GABA (Supplementary Fig. S4). Neither the amplitude nor frequency of the mIPSCs changed significantly, suggesting the lack of synaptic GABA_A receptor activation/desensitisation and the lack of an effect on GABA release probability, respectively.

Because of efficient GABA uptake, the tonic GABA_A current is either absent in pyramidal cells or significantly smaller than that in interneurons^{4,6}. Ambient GABA, however, can increase tonic GABA_A current in these cells. Indeed, 1, 5 and $50 \mu\text{M}$ GABA produced a dose-dependent increase in the tonic GABA_A current (Fig. 4c). This increase was two orders of magnitude larger than the change in the time-averaged current mediated by sIPSCs (I_{spont}), which was calculated as mean charge transfer of sIPSCs multiplied by their frequency⁶ (Fig. 4d). Thus, the overall effect of bath-applied GABA on the excitability of CA1 pyramidal neurons was dominated by tonic inhibition (Discussion). We next investigated the conditions under which ambient GABA is decreased.

Reduced tonic conductance correlates with low firing rate. We used a mouse lacking one of the two major GABA synthesizing enzymes, 65 kDa glutamic acid decarboxylase (GAD65^{-/-}).

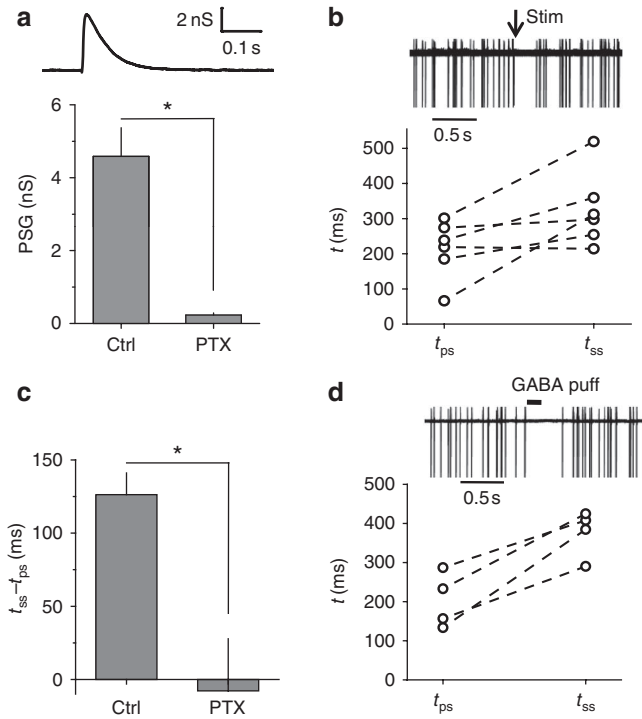


Figure 3 | Evoked GABA_A PSG and 100 μM GABA puff are inhibitory.

(a) Top: sample trace of calculated GABA_A mediated PSG. Bottom, Summary plot of averaged peak PSG in control (ctrl) and in 100 μM picrotoxin (PTX) ($n=7$). (b) Top: Five superimposed cell-attached recordings with synaptic stimulation (arrow). Bottom: Plot of averaged preceding spike (t_{ps}) and succeeding spike (t_{ss}) intervals in 6 individual cells. (c) Difference between t_{ss} and t_{ps} in control (ctrl) and in 100 μM picrotoxin (PTX) ($n=5$). (d) Top: 5 superimposed cell-attached recordings with 100 μM GABA puff. Bottom: plot of averaged preceding spike (t_{ps}) and succeeding spike (t_{ss}) intervals in four individual cells. Error bars, s.e.m., * $P<0.05$, paired t -test.

This mouse develops an ambient GABA deficit in the brain after the first month of life^{36,37}. Consistent with the reduced extracellular GABA, the tonic GABA_A current density was two times smaller in CA1 *str. radiatum* interneurons of GAD65^{-/-} mice than in wild-type (WT) mice interneurons (GAD65^{-/-}, $1.5 \pm 0.3 \times 10^5$ pA cm⁻², $n=7$ versus WT, $3.2 \pm 0.6 \times 10^5$ pA cm⁻², $n=10$; $P=0.037$; Fig. 5a,b). Surprisingly, we detected no difference in the magnitude of the tonic currents between the WT and GAD65^{-/-} CA1 pyramidal neurons (Fig. 5c,d). It is possible that under baseline conditions, ambient GABA does not reach the receptors on these cells⁶ and the small tonic current is mediated by agonist-independent spontaneous openings of GABA_A receptors^{38,39}.

GABA (5 μM) induced a similar rise in the holding current in GAD65^{-/-} and WT interneurons, indicating that the smaller tonic current in knockout animals was not due to a change in their sensitivity to ambient GABA (Fig. 6a,b). Consistent with our previous report⁶, 100 nM zolpidem, a benzodiazepine site agonist, enhanced the tonic GABA_A current and increased the sIPSC decay time in WT interneurons, suggesting that these currents were mediated by $\gamma 2$ -subunit-containing GABA_A receptors (Fig. 6c–f). Zolpidem had a similar effect in GAD65^{-/-} interneurons, pointing to an unchanged pharmacological profile of GABA_A receptors in these animals⁴⁰. Also consistent with a previous report⁴¹, the amplitude, kinetics and frequency of mIPSCs was not significantly different in GAD65^{-/-} interneurons compared with WT interneurons (Supplementary Fig. S5), suggesting that synaptic signalling was intact under resting conditions. This finding does not exclude, however,

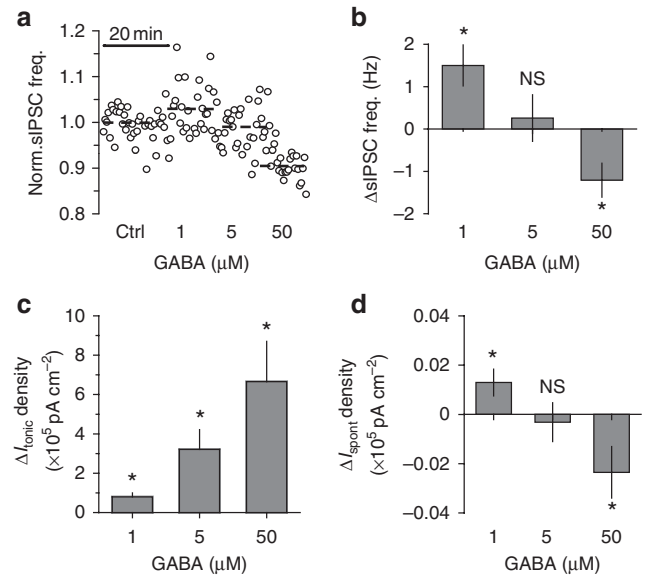


Figure 4 | Effect of ambient GABA on sIPSC and tonic current in CA1 pyramidal neurons.

(a) Normalized sIPSC frequency in CA1 pyramidal neuron in control (ctrl) and after application of 1, 5 and 50 μM GABA. (b) Summary plot of the change in sIPSC frequency induced by GABA ($n=11$ for 1 μM GABA, $n=9$ for 5 μM GABA, $n=6$ for 50 μM GABA). (c) Summary plot of the change in tonic GABA_A current (ΔI_{tonic}) density recorded in 1, 5 and 50 μM GABA ($n=10$). (d) Summary plot of the change in time-averaged phasic current (ΔI_{spont}) density recorded in 1, 5 and 50 μM GABA ($n=10$). Error bars, s.e.m., * $P<0.05$, NS $P>0.05$, paired t -test.

the possibility that synaptic GABA_A signalling differs between the two genotypes during sustained synaptic activation induced by prolonged electrical stimulation, as previously reported⁴¹. Because we did not deliver prolonged stimulation to the slices, this phenomenon is unlikely to contribute to the difference in the tonic currents.

In contrast to GABA_A receptor knockout animals⁴², we found no changes in the non-GABA-mediated holding current in GAD65^{-/-} interneurons, which suggests a lack of compensatory changes in the resting membrane conductances (Fig. 7a). The RMP (-70.6 ± 2.5 mV, $n=5$) and E_{GABA} (-59.2 ± 1.8 mV, $n=5$, $P=0.039$ compared with RMP, paired t -test) in GAD65^{-/-} interneurons were not significantly different from the RMP and E_{GABA} in WT cells.

Consistent with the excitatory effect of baseline tonic GABA_A conductance, the firing frequency of GAD65^{-/-} interneurons (0.023 ± 0.01 Hz, $n=7$) was significantly lower than that of WT cells (3.2 ± 0.7 Hz, $n=7$; $P<0.001$ compared with WT) (Fig. 7b,c). When GABA_A receptors were blocked, the excitability of the GAD65^{-/-} interneurons was not different from the WT cells, ruling out the possibility that compensatory changes were responsible for the reduced firing rate of these cells (Fig. 7d). If a reduced firing rate of GAD65^{-/-} interneurons results from the decreased tonic GABA_A conductance, exogenous GABA should rescue it. Indeed, bath application of 1 μM GABA increased the firing rate of GAD65^{-/-} interneurons by 0.8 ± 0.3 Hz ($n=6$, $P=0.015$ paired t -test). In contrast to WT interneurons, 5 μM GABA further increased the firing rate of GAD65^{-/-} interneurons by 3.5 ± 1.5 Hz ($n=7$, $P=0.03$ paired t -test; Fig. 7e,f). This effect was due to lower baseline tonic conductance in GAD65^{-/-} (0.31 ± 0.12 nS, $n=9$) than that in WT (0.62 ± 0.16 nS, $n=7$, $P=0.042$ for difference with GAD65^{-/-}) interneurons. Both 1 and 5 μM GABA resulted in an increase in tonic conductance (Δg_{GABA} , 0.48 ± 0.07 nS, $n=9$ and 1.07 ± 0.15 nS, $n=9$, respectively) within the range of excitatory GABA action (Fig. 1g). This finding further supports the notion that the decreased firing rates of GAD65^{-/-} interneurons are due to decreased tonic GABA_A excitation.

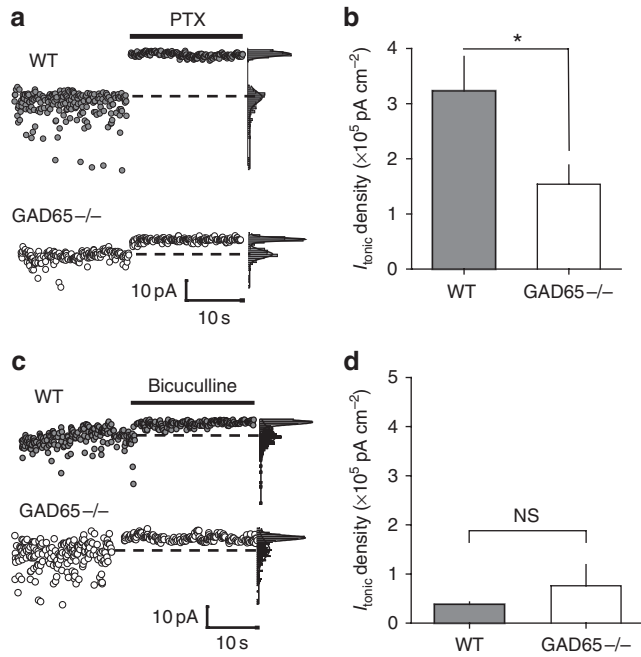


Figure 5 | Tonic GABA_A current in GAD65^{-/-} interneurons and pyramidal cells. (a) Change in I_{hold} in WT and GAD65^{-/-} interneurons produced by 100 μM picrotoxin (PTX). Right panels: Current histograms with Gaussian fits of recorded current. Dashed lines indicate the I_{hold} obtained from the peaks of the fits. (b) Summary plot of tonic GABA_A current (I_{tonic}) density in interneurons ($n=7$ for GAD65^{-/-}, $n=10$ for WT). (c) Change in I_{hold} in WT and GAD65^{-/-} pyramidal cells produced by 10 μM bicuculline. Right panels: same as in a. (d) Summary plot of tonic GABA_A current (I_{tonic}) density in WT ($n=6$) and GAD65^{-/-} ($n=4$) pyramidal cells. Error bars, s.e.m., NS $P>0.05$, * $P<0.05$, unpaired t -test.

We then compared the baseline frequency of spontaneous action potential-dependent IPSCs (aIPSCs = sIPSCs—mIPSCs) in WT and GAD65^{-/-} neurons to estimate the effect of an ambient GABA deficit on synaptic GABA_A signalling driven by interneuron firing. Consistent with interneuron firing rates, the frequency of aIPSCs in WT pyramidal cells (1.2 ± 0.4 Hz, $n=4$) was significantly higher than the frequency of the practically absent aIPSCs in GAD65^{-/-} pyramidal cells (0.1 ± 0.4 Hz, $n=6$, $P=0.041$ compared to WT; Fig. 8a). A similar difference in the frequency of the aIPSCs was observed in the interneurons (WT, 1.1 ± 0.3 Hz, $n=13$; GAD65^{-/-}, -0.1 ± 0.5 Hz, $n=9$, $P=0.013$; Fig. 8b).

Exogenous GABA increased the frequency of sIPSCs in GAD65^{-/-} pyramidal cells (1 μM , by 1.15 ± 0.05 Hz, $n=8$, $P<0.001$ paired t -test, and 5 μM , by 1.13 ± 0.04 Hz, $n=6$, $P<0.001$ paired t -test, Fig. 8c,d). Interestingly, this increase in the frequency of sIPSCs was not proportional to the increase in GAD65^{-/-} interneuron firing, whereas 5 μM GABA increased firing frequency several times more than 1 μM (Fig. 7e,f). There are at least two explanations for such a discrepancy. First, using somatic recordings, we were unable to detect sIPSCs from distal dendrites, and thus the frequency change might be underestimated. Second, interneurons target both pyramidal cells and other interneurons. The output of interconnected interneurons to pyramidal cells might not exactly follow the average firing rate of individual interneurons recorded in the *str. radiatum*. These considerations point to the complexity of the interneuron network and the need for future studies to dissect the effect of tonic excitation on different classes of interneurons. The present data, however, are sufficient to draw the general conclusion that resting levels of ambient GABA are set to maintain the tone of synaptic GABA-mediated signalling in the hippocampal CA1 region.

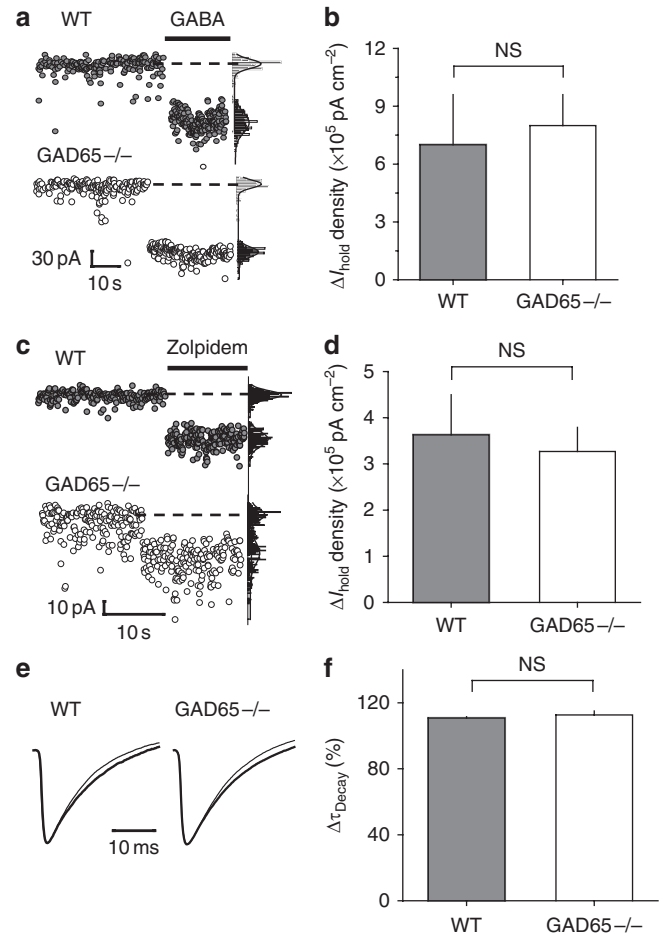


Figure 6 | WT and GAD65^{-/-} interneurons equally respond to 5 μM GABA and 100 nM zolpidem. (a) Change in I_{hold} in WT and GAD65^{-/-} interneurons produced by 5 μM GABA. Right panels: current histograms with Gaussian fits of recorded current. Dashed lines indicate the I_{hold} obtained from the peaks of the fits. (b) Summary plot of the change in I_{hold} density induced by 5 μM GABA in WT ($n=10$) and GAD65^{-/-} ($n=5$) interneurons. (c) Change in I_{hold} in WT and GAD65^{-/-} interneurons produced by 100 nM zolpidem. Right panels: same as in a. (d) Summary plot of the change in I_{hold} density induced by zolpidem in WT ($n=7$) and GAD65^{-/-} ($n=7$) interneurons. (e) Mean peak scaled sIPSCs recorded from WT and GAD65^{-/-} interneurons without (thin trace) or with 100 nM zolpidem (thick trace). (f) Summary plot of the change in the sIPSC decay time constant (τ_{decay}) induced by zolpidem in WT ($n=7$) and GAD65^{-/-} ($n=7$) interneurons. Error bars, s.e.m., NS $P>0.05$, unpaired t -test.

Discussion

Changes in extracellular GABA determine the magnitude of tonic GABA_A conductance, which has a biphasic effect on the excitability of hippocampal interneurons. A low-tonic GABA_A conductance depolarizes the cell and results in the onset of cell firing. This depolarization also enhances voltage-dependent RMP fluctuations, which are driven by stochastic Na⁺ channel opening²⁹. It is likely that these fluctuations are involved in the increase in the cell firing rate, because they get larger following GABA_A-mediated depolarization. When the tonic GABA_A conductance increases, the excitatory effect of depolarization is overpowered by inhibition. Both cell firing frequency and RMP fluctuations decrease. This inhibition can be explained by the shunting effect, which increases with the tonic GABA_A conductance.

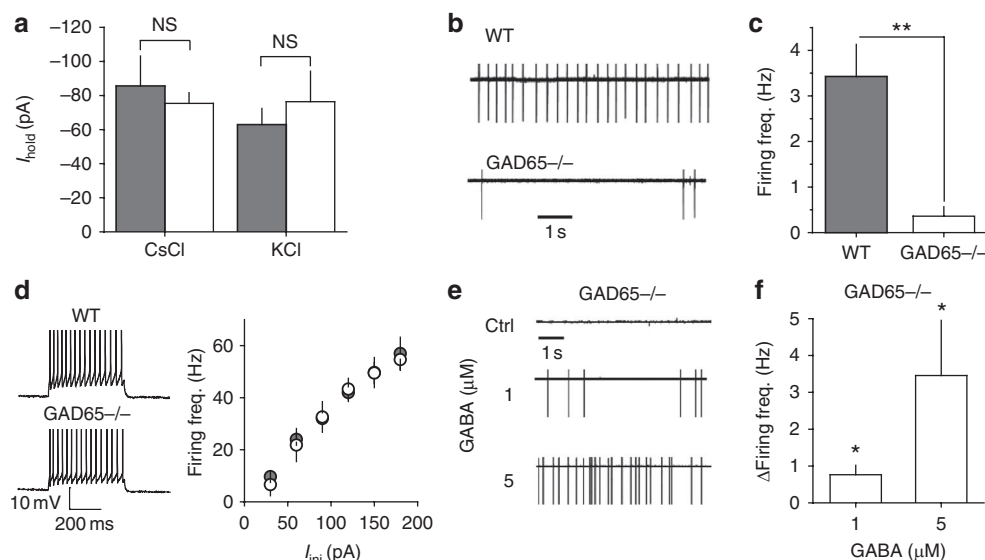


Figure 7 | Analysis of $GAD65^{-/-}$ interneurons. (a) Summary of I_{hold} recorded in WT (shaded columns) and $GAD65^{-/-}$ (open columns) interneurons voltage-clamped at -60 mV loaded with CsCl ($GAD65^{-/-}$ $n=8$; WT $n=13$) and with KCl ($GAD65^{-/-}$ $n=5$; WT $n=7$) in the presence of $100 \mu\text{M}$ picrotoxin. (b) Cell-attached recordings from WT and $GAD65^{-/-}$ interneurons (without picrotoxin). (c) Summary plot of firing frequency in WT and $GAD65^{-/-}$ interneurons ($n=7$) obtained under the same conditions as for b. (d) Left panel: Action potentials recorded in response to depolarizing current steps (90 pA; 500 ms) in whole-cell current-clamp mode from WT and $GAD65^{-/-}$ interneurons in the presence of $100 \mu\text{M}$ picrotoxin. Right panel: Summary plot of action potential frequency recorded during depolarizing steps varying from 30 to 180 pA (input-output characteristics) in $GAD65^{-/-}$ ($n=5$) and WT ($n=4$) interneurons. (e) Cell-attached recordings from $GAD65^{-/-}$ interneuron in control (ctrl) and in 1 and $5 \mu\text{M}$ GABA (without picrotoxin). (f) Summary plot of the change in firing frequency induced by GABA in $GAD65^{-/-}$ interneurons obtained under the same conditions as for e. Error bars, s.e.m., $^{**}P < 0.005$, $^{*}P < 0.05$, NS $P > 0.05$, unpaired (a and c) and paired (f) t -test.

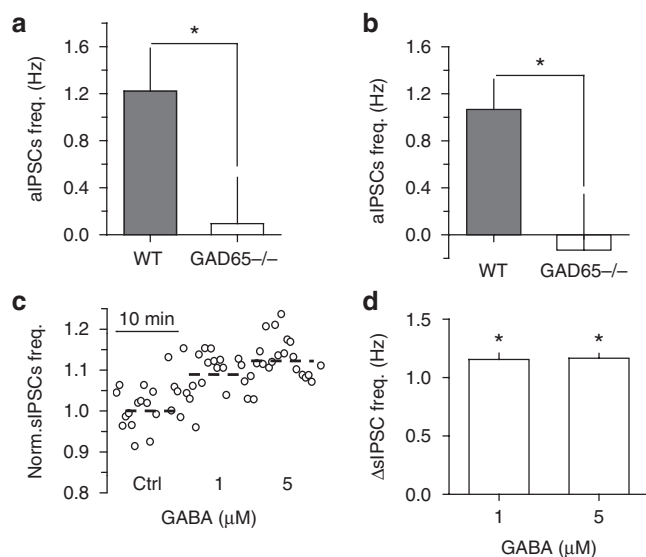


Figure 8 | $GABA_A$ mediated synaptic signalling in $GAD65^{-/-}$ CA1 neurons. (a, b) Summary plots of aIPSCs frequency in WT and $GAD65^{-/-}$ pyramidal cells ($n=4$ for WT, $n=6$ for $GAD65^{-/-}$) and interneurons ($n=13$ for WT, $n=9$ for $GAD65^{-/-}$), respectively. (c) Normalized sIPSC frequency in $GAD65^{-/-}$ pyramidal neuron in control (ctrl) and after 1 and $5 \mu\text{M}$ GABA application. (d) Summary plot of the change in sIPSC frequency by GABA in $GAD65^{-/-}$ pyramidal cells ($n=8$ for $1 \mu\text{M}$ GABA, $n=6$ for $5 \mu\text{M}$ GABA). Error bars, s.e.m., $^{*}P < 0.05$, unpaired (a, b) and paired (d) t -test.

Consistent with the effect of shunting, evoked synaptic $GABA_A$ signalling was inhibitory in interneurons, because of the large peak conductance. This finding, however, does not rule out the possible

excitatory effect of relatively small spontaneous $GABA_A$ -mediated postsynaptic currents. Nevertheless, the present finding adds one more distinction to the functional role of tonic and phasic $GABA_A$ -mediated signalling in the brain¹⁻³.

A biphasic effect of tonic $GABA_A$ conductance on neuronal firing has important implications for computation within a neuronal network. The classic view holds that neurons generate a variable output in response to the integration of synaptic inputs. Here we show that hippocampal interneurons can generate a variable output in response to changes in extrasynaptic GABA, regardless of excitatory synaptic drive. Because these neurons are part of the local circuit, extrasynaptic input can be considered as one of the inputs into the local neuronal network that determines the network operation and output.

An increase in ambient GABA has been reported for particular types of behaviour (for example, exploration¹¹) or in pathological conditions^{10,12}. We used bath application of GABA to mimic such an increase. Exogenous GABA, however, also induced a dose-dependent tonic current with a magnitude of two orders larger than the time-averaged current produced by the change in sIPSCs in CA1 pyramidal neurons. Because these cells are reported to have hyperpolarizing E_{GABA} (ref. 17), the tonic $GABA_A$ current may be their main source of inhibition. This raises the question of whether a biphasic change in sIPSC frequency is of any importance for the excitability of pyramidal neurons. In fact, bath application of GABA may not faithfully reproduce the changes in ambient GABA concentrations under physiological conditions. A recent report using an innovative GABA imaging technique demonstrated layer-specific changes in ambient GABA resulting from increased neuronal activity⁴³. Moreover, the functional roles of tonic and phasic $GABA_A$ signalling are largely different^{2,30}. For example, tonic $GABA_A$ conductance determines the membrane time constant and characteristic length constant³⁰, and modulates neuronal offset in CA1 pyramidal neurons⁴⁴. $GABA_A$ -mediated IPSCs interact in a time-dependent manner with glutamatergic EPSCs, which has a specific impact on neuronal

computation (for example, integration time window of neuronal inputs⁴⁵), and are involved in network synchronization and oscillatory behaviour⁴⁶. Thus, the actual effect of physiological changes in ambient GABA concentration on the hippocampal network function requires further investigation.

In summary, we suggest that the described phenomenon has a role in different types of excitable cells. The amount of conductance acts to switch between excitation and inhibition when certain conditions are met: the current has low depolarizing reversal potential and the produced depolarization is amplified by other voltage-dependent conductances. Here we demonstrated these conditions in hippocampal interneurons, but they can be potentially observed in the other neurons with depolarizing E_{GABA} (refs 9,22–25). It is also likely that E_{GABA} determines the excitation peak conductance and the inhibitory threshold conductance. Thus, the biphasic action of tonic GABA_A conductance should be considered in the broader context of the determinants of E_{GABA} . First, the expression of the main Cl⁻ transporters (NKCC1 and KCC2) is developmentally regulated, which differs in various cell types. For example, in hippocampal pyramidal neurons, the ratio of KCC2/NKCC1 increases during development, making GABA hyperpolarizing¹⁴. In contrast, this ratio is fixed in hippocampal interneurons and GABA continues to have depolarizing effects throughout development¹⁹. Second, activity-dependent regulation of Cl⁻ transporters contributes to E_{GABA} in different cells. A recent report demonstrated that NMDA receptor activity downregulates KCC2, resulting in a depolarizing GABA_A-mediated current in rat dissociated neurons⁴⁷.

Additionally, the described phenomenon can have a role at subcellular level. We did not systematically investigate the effect of low GABA concentrations at different sites within interneurons. A previous report, however, demonstrated that depolarizing GABA can produce inhibition in the soma and excitation in dendrites of cortical pyramidal cells⁴⁸. This can be explained that shunting inhibition of the axon initial segment is larger for soma than for more remote dendritic sites. That is, the inhibitory threshold conductance increases with distance from the axon initial segment. This observation prompts further investigation of tonic GABA_A conductances at the subcellular level.

Methods

Electrophysiology in hippocampal slices. All experimental procedures were performed in accordance with the guidelines of the Animal Experiment Committee of the RIKEN Brain Science Institute. Hippocampal slices (350–380 μm) were obtained from 4- to 6-week-old male WT or GAD65^{-/-} littermates⁴⁹. Heterozygous knockout mice with a C57BL/6J genetic background were interbred to produce WT and GAD65^{-/-} mice in a specific pathogen-free facility. Mice were housed at 24 °C with a 12/12-h light/dark cycle and *ad libitum* access to food and water. Genomic PCR was used to differentiate the mice.

Hippocampal slices were maintained at room temperature in a submerged chamber with solution containing (in mM): 119 NaCl, 2.5 KCl, 1.3 MgSO₄, 1 CaCl₂, 26.2 NaHCO₃, 1 NaH₂PO₄, and 11 glucose, and saturated with 95% CO₂/5% O₂. After 1 h of incubation, slices were transferred to the recording chamber and superfused at 34 °C with the solution described above, but containing 2.5 mM CaCl₂. Except for the experiment shown in Supplementary Figure S1, AMPA/kainate, NMDA, and GABA_B receptors were blocked with 25 μM NBQX, 50 μM APV, and 5 μM CGP 52432 (Tocris Cookson), respectively.

CA1 pyramidal cells and *str. radiatum* interneurons were visually identified with an infrared differential interference contrast microscope (Olympus BX51WI). The data were acquired with a Multiclamp700B (Axon Instruments), filtered at 2 kHz, and digitized at 5 kHz using a NI PCI-6221 data acquisition card (National Instruments). The data were analysed without further re-sampling. Sample traces were also taken at the same rate, except for the long traces (> 30 s), which were re-sampled at 10 Hz. Whole-cell, gramicidin-perforated patch, and cell-attached recordings were performed in separate cells.

Whole-cell experiments. Whole-cell pipettes used in voltage-clamp recordings contained (in mM): 130 CsCl, 8 NaCl, 10 Cs-HEPES, 2 EGTA, 0.2 MgCl₂, 2 MgATP, 0.3 Na₃GTP, and 5 QX314Br (pH 7.2, osmolarity 295 mOsm, liquid junction potential 4.1 mV). In the experiments for Figure 7a, KCl was used instead of CsCl (liquid junction potential 3.4 mV). Whole-cell current-clamp recordings were performed with pipettes containing (in mM): 132.3 K-gluconate, 7.7 KCl, 4 NaCl, 0.5 CaCl₂, 10 HEPES, 5 EGTA, 2 MgATP, and 0.5 Na₃GTP.

Series resistance (R_s), input resistance (R_i), and membrane capacitance (c_m) were monitored throughout the recordings. These parameters were obtained from the current in response to hyperpolarizing voltage steps ($V_{step} = -5$ mV).

$$R_s = V_{step} / I_{peak} \quad (1)$$

$$R_i = V_{step} / I_{ss} - R_s \quad (2)$$

$$c_m = \tau(1/R_s + 1/R_i) \quad (3)$$

where, I_{peak} is the peak amplitude of the current transient immediately after the step is applied, τ is the decay time constant of the current, and I_{ss} is the steady-state current⁵⁰. The R_s was not compensated and data were discarded if R_s changed by more than 20% during the recording. There was no significant difference in c_m between GAD65^{-/-} (70.9 ± 7.9 pF, $n = 9$) and WT (69.4 ± 6.9 pF, $n = 11$) interneurons ($P = 0.445$).

Tonic GABA_A current (I_{tonic}) was calculated as the difference between the baseline I_{hold} and the I_{hold} in the presence of a GABA_A receptor antagonist. The change in the tonic GABA_A current (ΔI_{tonic}) was calculated as the difference between the baseline I_{hold} and the I_{hold} in the presence of exogenous GABA. I_{tonic} density was obtained by dividing I_{tonic} by the surface area of the neuron. The surface area was obtained by dividing c_m by the membrane capacitance constant (0.9 μF cm⁻²)⁵⁰. Tonic GABA_A conductance was calculated as the difference between the baseline conductance ($1/R_s$) and the conductance in the presence of a GABA_A receptor antagonist (g_{GABA}) or exogenous GABA (Δg_{GABA}).

Synaptic GABA_A conductance in response to electric stimulation (PSG, Fig. 3a) was calculated according to

$$PSG = PSC / (E_{GABA} - V_{hold}) \quad (4)$$

where PSC—postsynaptic current in the presence of ionotropic glutamate and GABA_B receptor antagonists; $V_{hold} = 70$ mV—holding current; $E_{GABA} = -0.7$ mV was calculated by

$$E_{GABA} = -\frac{RT}{F} \ln \frac{P_{Cl} [Cl^-]_o + P_{HCO_3} [HCO_3^-]_o}{P_{Cl} [Cl^-]_i + P_{HCO_3} [HCO_3^-]_i} \quad (5)$$

where $P_{Cl} = 1$ and $P_{HCO_3} = 0.2$ —relative permeabilities for Cl⁻ and HCO₃⁻, respectively⁵¹.

mIPSCs were recorded in the presence of 1 μM tetrodotoxin. sIPSCs and mIPSCs were completely blocked by 100 μM picrotoxin. Frequency, mean amplitude, and decay time constant of sIPSCs and mIPSCs were analysed off-line with the MiniAnalysis (Synaptosoft) and Clampfit (MDS Analytical Technologies). aIPSC frequency was calculated as the difference between the sIPSC and mIPSC frequencies. Time-averaged current mediated by sIPSCs (I_{spont}) was calculated as the mean charge transfer of sIPSCs multiplied by their frequency⁶.

Gramicidin-perforated patch experiments. The pipette tips were filled with the solution containing (in mM) 145 KCl, 10 HEPES, 5 ATP-Mg, 0.2 GTP-Na, 2 QX314, and 2 EGTA to prevent leakage of the antibiotic while approaching the cell. The pipettes were back-filled with the same solution that also contained 20 μg ml⁻¹ gramicidin-D (Sigma). Fresh gramicidin solution was made every 2 h. After the pipette tip contacted the cell membrane, the R_s was monitored. Recordings were started when the R_s stabilized at 30–45 MΩ (usually within 15–20 min). All measurements were corrected for a liquid junction potential and voltage drop across the R_s (ref. 52). RMP was measured in current clamp mode (I_{hold} was 0 pA). Mean RMP and its standard deviation were obtained under control conditions and in the presence of GABA. The depolarizing effect of GABA was calculated as difference between mean RMPs. In some experiments, the cells were voltage-clamped at -65 mV. Membrane I-V characteristics were then obtained with 2,000-ms voltage steps delivered from -90 to -70 mV with 10 mV intervals, and from -55 to -20 mV with 5-mV intervals. I-V characteristics for GABA_A tonic current were obtained as the difference between membrane I-V characteristics in 5 μM GABA and in 100 μM picrotoxin, added sequentially.

Cell-attached experiments. Pipettes were filled with superfusion solution and loosely attached to the cell membrane to measure interneuron firing without perturbing intracellular ionic concentrations. Recordings were performed in the voltage-clamp mode from the interneurons in which action currents were detectable (approximately 50% of cells)^{21,27}. The command potential was set to the potential at which the holding current was 0 pA to avoid direct cell stimulation by the electrode⁵³. The evoked GABA_A-mediated PSGs were triggered by 200-μs current pulses at 50 μA delivered by a tungsten monopolar electrode placed in the *str. radiatum*. GABA_A activation was also produced with a 100-μM GABA puff (100 ms, 50 psi). Preceding (t_p) and succeeding (t_s) spike intervals were calculated from the beginning of the synaptic stimulation or GABA puff.

Computational model. The cylindrical neuron (length 20 μm; diameter 10 μm; total surface 628 μm²) was created with the Neuron 7 simulator. The cell excitability was described according to Hodgkin-Huxley's model with corresponding Na⁺ (Na_v) and K⁺ (K_v) channels (single-channel conductance: $\gamma_{Na} = 20$ pS and

$\gamma_K = 15$ pS; channel density: 50 and $0.667 \mu\text{m}^{-2}$, giving a total number of channels of $N_{Na} = 31,400$ and $N_K = 419$. Additionally, A-type K^+ channels (K_A) were introduced (single-channel conductance $\gamma_{KA} = 10$ pS; channel density: $8 \mu\text{m}^{-2}$ giving total number of channels: $N_{KA} = 5,024$)³⁴. The transition of the channels between different conformational states was described as a Markov process, whereas the rate constants varied with the voltage^{54,55}. The membrane also included the linear deterministic tonic GABA_A conductance (g_{GABA}), which was varied from 0 to 0.2 mS cm^{-2} with 0.001 mS cm^{-2} steps. On the basis of this set of conductances, we used the following equation:

$$C_m \frac{dV}{dt} = I_{inj} - g_{Na}(V - E_{Na}) - g_{Kv}(V - E_K) - g_{KA}(V - E_K) - g_{GABA}(V - E_{GABA}) \quad (6)$$

where C_m —membrane capacitance ($1 \mu\text{F cm}^{-2}$), I_{inj} —injected current (0 pA for baseline conditions), E_{Na} — Na^+ equilibrium potential (50 mV), and E_K — K^+ equilibrium potential (-77 mV). The reversal potential for GABA_A current ($E_{GABA} = -55$ mV) was set 10.2 mV above the mean RMP without GABA_A conductance (65.2 mV) to match experimental data. g_{Na} , g_K , and g_{KA} — Na_v , K_v , and K_A conductances, respectively, were controlled by continuous variables that range between 0 and 1 (m, h, n, k, l).

$$g_{Na} = N_{Na} \gamma_{Na} [m_3 h_1], \quad (7)$$

$$g_K = N_K \gamma_K [n_4], \quad (8)$$

$$g_{KA} = N_{KA} \gamma_{KA} [l_1 k_1], \quad (9)$$

where $[m_3 h_1]$, $[n_4]$, and $[l_1 k_1]$ are the probabilities of the Na_v , K_v , and K_A channels to be in the open state according to their respective kinetic schemes^{54,55}. The variables m, h, n, k, l obeyed first-order differential equations with voltage dependent rate constants ($\alpha_m, \beta_m, \alpha_h, \beta_h, \alpha_n, \beta_n, \alpha_k, \beta_k, \alpha_l$).

$$\frac{dm}{dt} = \alpha_m(1 - m) - \beta_m m \quad (10)$$

$$\alpha_m = -\frac{0.1(V + 40)}{\exp\left(-\frac{V + 40}{10}\right) - 1} \quad (11)$$

$$\beta_m = \frac{4 \exp(-V - 65)}{18} \quad (12)$$

$$\frac{dh}{dt} = \alpha_h(1 - h) - \beta_h h \quad (13)$$

$$\alpha_h = 0.07 \exp\left(-\frac{65 + V}{20}\right) \quad (14)$$

$$\beta_h = \frac{1}{1 + \exp\left(-\frac{35 + V}{5}\right)} \quad (15)$$

$$\frac{dn}{dt} = \alpha_n(1 - n) - \beta_n n \quad (16)$$

$$\alpha_n = -\frac{0.01(55 + V)}{\exp\left(-\frac{55 + V}{10}\right) - 1} \quad (17)$$

$$\beta_n = 0.125 \exp\left(-\frac{65 + V}{80}\right) \quad (18)$$

$$\frac{dk}{dt} = \alpha_k(1 - k) - \beta_k k \quad (19)$$

$$\alpha_k = \exp\left(-0.038 \left(1.5 + \frac{1}{1 + \frac{\exp(V + 40)}{5}}\right) (V - 11)\right) \quad (20)$$

$$\beta_k = \exp\left(-0.038 \left(-0.825 + \frac{1}{1 + \frac{\exp(V + 40)}{5}}\right) (V - 11)\right) \quad (21)$$

$$\frac{dl}{dt} = \alpha_l(1 - l) \quad (22)$$

$$\alpha_l = \exp(0.11(V + 56)) \quad (23)$$

The effect of g_{GABA} on fluctuations of RMP (RMP standard deviation) was studied when the density of Na^+ channels was reduced from 50 to $25 \mu\text{m}^{-2}$ to prevent action potential generation.

The effect of membrane depolarization on the cell firing and the RMP fluctuations was studied with the current injections (I_{inj}) from 0 to 1 nA and $g_{GABA} = 0$ nS.

All simulations were run for 1,000 ms, and the data were collected from the interval between 500 ms and 1,000 ms when the model reached a quasi-steady state. All the model data are means from 10 independent simulations. To avoid the correlation between data, each computation was performed with a different seed obtained from the random number generator.

Statistical analysis. Data are presented as means \pm s.e.m. Error bars on the graphs represent s.e.m. Statistical comparisons were made using unpaired Student's t -test unless a paired t -test is stated. A P -value of less than 0.05 was considered statistically significant.

References

- Glykys, J. & Mody, I. Activation of GABAA receptors: views from outside the synaptic cleft. *Neuron* **56**, 763–770 (2007).
- Farrant, M. & Nusser, Z. Variations on an inhibitory theme: phasic and tonic activation of GABA(A) receptors. *Nat. Rev. Neurosci.* **6**, 215–229 (2005).
- Semyanov, A., Walker, M. C., Kullmann, D. M. & Silver, R. A. Tonically active GABA A receptors: modulating gain and maintaining the tone. *Trends Neurosci.* **27**, 262–269 (2004).
- Scimemi, A., Semyanov, A., Sperk, G., Kullmann, D. M. & Walker, M. C. Multiple and plastic receptors mediate tonic GABAA receptor currents in the hippocampus. *J. Neurosci.* **25**, 10016–10024 (2005).
- Glykys, J., Mann, E. O. & Mody, I. Which GABA(A) receptor subunits are necessary for tonic inhibition in the hippocampus? *J. Neurosci.* **28**, 1421–1426 (2008).
- Semyanov, A., Walker, M. C. & Kullmann, D. M. GABA uptake regulates cortical excitability via cell type-specific tonic inhibition. *Nat. Neurosci.* **6**, 484–490 (2003).
- Jia, F. *et al.* An extrasynaptic GABAA receptor mediates tonic inhibition in thalamic VB neurons. *J. Neurophysiol.* **94**, 4491–4501 (2005).
- Vardya, I., Drasbek, K. R., Dosa, Z. & Jensen, K. Cell type-specific GABA A receptor-mediated tonic inhibition in mouse neocortex. *J. Neurophysiol.* **100**, 526–532 (2008).
- Ade, K. K., Janssen, M. J., Ortinski, P. I. & Vicini, S. Differential tonic GABA conductances in striatal medium spiny neurons. *J. Neurosci.* **28**, 1185–1197 (2008).
- Minamoto, Y. *et al.* *In vivo* microdialysis of amino acid neurotransmitters in the hippocampus in amygdaloid kindled rat. *Brain Res.* **573**, 345–348 (1992).
- Bianchi, L. *et al.* Investigation on acetylcholine, aspartate, glutamate and GABA extracellular levels from ventral hippocampus during repeated exploratory activity in the rat. *Neurochem. Res.* **28**, 565–573 (2003).
- Kupers, R., Danielsen, E. R., Kehlet, H., Christensen, R. & Thomsen, C. Painful tonic heat stimulation induces GABA accumulation in the prefrontal cortex in man. *Pain* **142**, 89–93 (2009).
- Dzhala, V. I. *et al.* NKCC1 transporter facilitates seizures in the developing brain. *Nat. Med.* **11**, 1205–1213 (2005).
- Rivera, C. *et al.* The K^+/Cl^- co-transporter KCC2 renders GABA hyperpolarizing during neuronal maturation. *Nature* **397**, 251–255 (1999).
- Hausselt, S. E., Euler, T., Detwiler, P. B. & Denk, W. A dendrite-autonomous mechanism for direction selectivity in retinal starburst amacrine cells. *PLoS Biol.* **5**, e185 (2007).
- Khiring, S. *et al.* GABAergic depolarization of the axon initial segment in cortical principal neurons is caused by the $\text{Na}^+/\text{K}^+/\text{2Cl}^-$ cotransporter NKCC1. *J. Neurosci.* **28**, 4635–4639 (2008).
- Glickfeld, L. L., Roberts, J. D., Somogyi, P. & Scanziani, M. Interneurons hyperpolarize pyramidal cells along their entire somatodendritic axis. *Nat. Neurosci.* **12**, 21–23 (2009).
- Michelson, H. B. & Wong, R. K. Excitatory synaptic responses mediated by GABAA receptors in the hippocampus. *Science* **253**, 1420–1423 (1991).
- Bank, T. G. & McBain, C. J. GABAergic input onto CA3 hippocampal interneurons remains shunting throughout development. *J. Neurosci.* **26**, 11720–11725 (2006).
- Vida, I., Bartos, M. & Jonas, P. Shunting inhibition improves robustness of gamma oscillations in hippocampal interneuron networks by homogenizing firing rates. *Neuron* **49**, 107–117 (2006).
- Verheugen, J. A., Fricker, D. & Miles, R. Noninvasive measurements of the membrane potential and GABAergic action in hippocampal interneurons. *J. Neurosci.* **19**, 2546–2555 (1999).

22. Chavas, J. & Marty, A. Coexistence of excitatory and inhibitory GABA synapses in the cerebellar interneuron network. *J. Neurosci.* **23**, 2019–2031 (2003).
23. Woodruff, A. R., Monyer, H. & Sah, P. GABAergic excitation in the basolateral amygdala. *J. Neurosci.* **26**, 11881–11887 (2006).
24. Bracci, E. & Panzeri, S. Excitatory GABAergic effects in striatal projection neurons. *J. Neurophysiol.* **95**, 1285–1290 (2006).
25. Bowerly, N. G. *et al.* Indirect effects of amino-acids on sympathetic ganglion cells mediated through the release of gamma-aminobutyric acid from glial cells. *Br. J. Pharmacol.* **57**, 73–91 (1976).
26. Morita, K., Tsumoto, K. & Aihara, K. Possible effects of depolarizing GABA_A conductance on the neuronal input-output relationship: a modeling study. *J. Neurophysiol.* **93**, 3504–3523 (2005).
27. Fricker, D., Verheugen, J. A. & Miles, R. Cell-attached measurements of the firing threshold of rat hippocampal neurones. *J. Physiol.* **517** (Part 3), 791–804 (1999).
28. Bourdeau, M. L., Morin, F., Laurent, C. E., Azzi, M. & Lacaille, J. C. Kv4.3-mediated A-type K⁺ currents underlie rhythmic activity in hippocampal interneurons. *J. Neurosci.* **27**, 1942–1953 (2007).
29. Chapman, C. A. & Lacaille, J. C. Intrinsic theta-frequency membrane potential oscillations in hippocampal CA1 interneurons of stratum lacunosum-moleculare. *J. Neurophysiol.* **81**, 1296–1307 (1999).
30. Walker, M. C. & Semyanov, A. Regulation of excitability by extrasynaptic GABA(A) receptors. *Results Probl. Cell Differ.* **44**, 29–48 (2008).
31. Brown, D. A. & Marsh, S. Axonal GABA-receptors in mammalian peripheral nerve trunks. *Brain Res.* **156**, 187–191 (1978).
32. Rojas, P., Akrouh, A., Eisenman, L. N. & Mennerick, S. Differential effects of axon initial segment and somatodendritic GABA_A receptors on excitability measures in rat dentate granule neurons. *J. Neurophysiol.* **105**, 366–379 (2011).
33. Morin, F., Haufler, D., Skinner, F. K. & Lacaille, J. C. Characterization of voltage-gated K⁺ currents contributing to subthreshold membrane potential oscillations in hippocampal CA1 interneurons. *J. Neurophysiol.* **103**, 3472–3489 (2010).
34. Migliore, M., Hoffman, D. A., Magee, J. C. & Johnston, D. Role of an A-type K⁺ conductance in the back-propagation of action potentials in the dendrites of hippocampal pyramidal neurons. *J. Comput. Neurosci.* **7**, 5–15 (1999).
35. Klausberger, T. & Somogyi, P. Neuronal diversity and temporal dynamics: the unity of hippocampal circuit operations. *Science* **321**, 53–57 (2008).
36. Kash, S. F. *et al.* Epilepsy in mice deficient in the 65-kDa isoform of glutamic acid decarboxylase. *Proc. Natl Acad. Sci. USA* **94**, 14060–14065 (1997).
37. Stork, O. *et al.* Postnatal development of a GABA deficit and disturbance of neural functions in mice lacking GAD65. *Brain Res.* **865**, 45–58 (2000).
38. Birnir, B., Everitt, A. B., Lim, M. S. & Gage, P. W. Spontaneously opening GABA(A) channels in CA1 pyramidal neurones of rat hippocampus. *J. Membr. Biol.* **174**, 21–29 (2000).
39. McCartney, M. R., Deeb, T. Z., Henderson, T. N. & Hales, T. G. Tonically active GABA_A receptors in hippocampal pyramidal neurons exhibit constitutive GABA-independent gating. *Mol. Pharmacol.* **71**, 539–548 (2007).
40. Kash, S. F., Tecott, L. H., Hodge, C. & Baekkeskov, S. Increased anxiety and altered responses to anxiolytics in mice deficient in the 65-kDa isoform of glutamic acid decarboxylase. *Proc. Natl Acad. Sci. USA* **96**, 1698–1703 (1999).
41. Tian, N. *et al.* The role of the synthetic enzyme GAD65 in the control of neuronal gamma-aminobutyric acid release. *Proc. Natl Acad. Sci. USA* **96**, 12911–12916 (1999).
42. Brickley, S. G., Revilla, V., Cull-Candy, S. G., Wisden, W. & Farrant, M. Adaptive regulation of neuronal excitability by a voltage-independent potassium conductance. *Nature* **409**, 88–92 (2001).
43. Morishima, T. *et al.* GABA imaging in brain slices using immobilized enzyme-linked photoanalysis. *Neurosci. Res.* **67**, 347–353 (2010).
44. Pavlov, I., Savtchenko, L. P., Kullmann, D. M., Semyanov, A. & Walker, M. C. Outwardly rectifying tonically active GABA_A receptors in pyramidal cells modulate neuronal offset, not gain. *J. Neurosci.* **29**, 15341–15350 (2009).
45. Pouille, F. & Scanziani, M. Enforcement of temporal fidelity in pyramidal cells by somatic feed-forward inhibition. *Science* **293**, 1159–1163 (2001).
46. Bartos, M., Vida, I. & Jonas, P. Synaptic mechanisms of synchronized gamma oscillations in inhibitory interneuron networks. *Nat. Rev. Neurosci.* **8**, 45–56 (2007).
47. Lee, H. H., Deeb, T. Z., Walker, J. A., Davies, P. A. & Moss, S. J. NMDA receptor activity downregulates KCC2 resulting in depolarizing GABA(A) receptor-mediated currents. *Nat. Neurosci.* **14**, 736–743 (2011).
48. Gullledge, A. T. & Stuart, G. J. Excitatory actions of GABA in the cortex. *Neuron* **37**, 299–309 (2003).
49. Asada, H. *et al.* Mice lacking the 65 kDa isoform of glutamic acid decarboxylase (GAD65) maintain normal levels of GAD67 and GABA in their brains but are susceptible to seizures. *Biochem. Biophys. Res. Commun.* **229**, 891–895 (1996).
50. Gentet, L. J., Stuart, G. J. & Clements, J. D. Direct measurement of specific membrane capacitance in neurons. *Biophys. J.* **79**, 314–320 (2000).
51. Kaila, K. Ionic basis of GABA_A receptor channel function in the nervous system. *Prog. Neurobiol.* **42**, 489–537 (1994).
52. Ulrich, D. & Huguenard, J. R. Nucleus-specific chloride homeostasis in rat thalamus. *J. Neurosci.* **17**, 2348–2354 (1997).
53. Perkins, K. L. Cell-attached voltage-clamp and current-clamp recording and stimulation techniques in brain slices. *J. Neurosci. Methods* **154**, 1–18 (2006).
54. DeFelice, L. J. & Isaac, A. Chaotic states in a random world: Relationship between the nonlinear differential equations of excitability and the stochastic properties of ion channels. *J. Stat. Phys.* **70**, 339–354 (1993).
55. Savtchenko, L. P., Gogan, P., Korogod, S. M. & Tyc-Dumont, S. Imaging stochastic spatial variability of active channel clusters during excitation of single neurons. *Neurosci. Res.* **39**, 431–446 (2001).

Acknowledgements

We thank Kunihiko Obata for providing us GAD65^{-/-} mice; Kaiyu Zheng for providing the multimode cluster for computations; Dimitri Kullmann, Matthew Walker, Hajime Hirase, Ivan Pavlov, Karri Lamsa, Thomas McHugh, Kirill Volynski, Stephen F. Heinemann, Dmitri Rusakov and all members of the AS laboratory for reading and commenting on the manuscript. This work was supported by RIKEN BSI and The Wellcome Trust.

Author contribution

A.S. and I.S. designed the study and planned the experiments; A.S., I.S., and L.S. analysed the data and prepared the manuscript; I.S. performed all the experiments; L.S. performed the modelling.

Additional information

Supplementary Information accompanies this paper at <http://www.nature.com/naturecommunications>

Competing financial interests: The authors declare no competing financial interests.

Reprints and permission information is available online at <http://npg.nature.com/reprintsandpermissions/>

How to cite this article: Song, I. *et al.* Tonic excitation or inhibition is set by GABA_A conductance in hippocampal interneurons. *Nat. Commun.* **2**:376 doi: 10.1038/ncomms1377 (2011).

License: This work is licensed under a Creative Commons Attribution-NonCommercial-Share Alike 3.0 Unported License. To view a copy of this license, visit <http://creativecommons.org/licenses/by-nc-sa/3.0/>